in Proc. IEEE PIMRC-02, Lisbon (Portugal), Sept. 2002, pp. 1012–1016

PULSE-SHAPING OFDM/BFDM SYSTEMS FOR TIME-VARYING CHANNELS: ISI/ICI ANALYSIS, OPTIMAL PULSE DESIGN, AND EFFICIENT IMPLEMENTATION

Dieter Schafhuber, Gerald Matz, and Franz Hlawatsch

Institute of Communications and Radio-Frequency Engineering, Vienna University of Technology
Gusshausstrasse 25/389, A-1040 Vienna, Austria
phone: +43 1 58801 38973, fax: +43 1 58801 38999, email: Dieter.Schafhuber@ieee.org
web: http://www.nt.tuwien.ac.at/dspgroup/time.html

ABSTRACT

This paper considers practically relevant aspects and advantages of *pulse-shaping* orthogonal/biorthogonal frequency division multiplexing (OFDM/BFDM) systems. We analyze the intersymbol/intercarrier interference (ISI/ICI) in such systems when they operate over time-varying channels. Two methods for an ISI/ICI-minimizing pulse design are proposed, and efficient FFT-based modulator and demodulator implementations are presented. Simulations show that for fast time-varying channels, optimized BFDM systems can outperform conventional OFDM systems with respect to ISI/ICI.

1. INTRODUCTION

Background. *Orthogonal frequency division multiplexing* (OFDM) is an attractive modulation scheme for high data-rate wireless communications [1–3]. Conventional OFDM, which employs rectangular transmit/receive pulses and a cyclic prefix (CP-OFDM) [2], is part of the standards IEEE 802.11a, Hiperlan/2, DAB-T, and DVB-T and is being considered for broadband wireless access by the IEEE 802.16 standardization work group. OFDM is also a promising candidate for future cellular communication systems.

Pulse-shaping OFDM systems and *biorthogonal frequency division multiplexing* (BFDM) systems [4–8] have several potential advantages over traditional CP-OFDM systems: higher bandwidth efficiency [4]; reduced sensitivity to carrier frequency offsets [5], oscillator phase noise, and narrowband interference; and reduced intersymbol/intercarrier interference (ISI/ICI) [4]. Less ISI/ICI will be important for future communication systems where Doppler frequencies will be larger (equivalently, channel variations will be faster) due to higher carrier frequencies and/or higher mobile velocities. On the other hand, a potential drawback of BFDM systems relative to OFDM systems is noise enhancement [4].

The design of "optimal" OFDM/BFDM transmit and receive pulses is a current research topic [4, 6–8]. However, to the authors' knowledge, performance results have been reported only for pulse-shaping OFDM/BFDM systems with spectral efficiencies ≤ 0.5. In contrast, practical CP-OFDM systems have spectral efficiencies ≥ 0.8. Also, it appears that no performance comparison of pulse-shaping OFDM/BFDM systems and CP-OFDM systems has been presented so far.

Funding by FWF grant P15156 and IST project ANTIUM.

Contributions and Organization. Following a presentation of the system model in Section 2, Section 3 provides both an exact analysis of as well as approximations and bounds for the ISI/ICI power in pulse-shaping OFDM/BFDM systems operating over time-varying channels. In Section 4, we present two methods for an optimal pulse design based on a minimization of the ISI/ICI power. Section 5 proposes efficient, FFT-based modulator and demodulator implementations whose complexity is only slightly larger than for CP-OFDM systems. Finally, simulation results are presented in Section 6. It is shown that for practically relevant spectral efficiencies, the ISI/ICI power of optimized BFDM systems can be smaller than that of CP-OFDM systems by about 3 dB.

2. SYSTEM MODEL

Modulator. We consider a pulse-shaping OFDM/BFDM system with K subcarriers, symbol duration T, and subcarrier frequency spacing F. Time-frequency translates $g_{l,k}(t) \triangleq g(t-lT)\,e^{j2\pi kF(t-lT)}$ of a transmit pulse $g(t)$ are used to form the equivalent baseband transmit signal

$$s(t) = \sum_{l=-\infty}^{\infty} \sum_{k=0}^{K-1} a_{l,k}\, g_{l,k}(t). \qquad (1)$$

Here, $a_{l,k}$ ($l \in \mathbb{Z}$, $k \in \{0,\ldots,K-1\}$) denotes the data symbol at symbol time l and subcarrier k. The symbols $a_{l,k}$ are assumed i.i.d. with zero mean and mean power $\mathrm{E}\{|a_{l,k}|^2\} = \sigma_a^2$.

Channel. Transmitting $s(t)$ over a random time-varying channel $\mathbb{H}$ with time-varying impulse response $h(t,\tau)$ [9,10] yields the received signal (integrals are from $-\infty$ to ∞)

$$r(t) = (\mathbb{H}s)(t) = \int_{\tau} h(t,\tau)\, s(t-\tau)\, d\tau.$$

(In this paper, we will consider only the noiseless case.) The channel $\mathbb{H}$ is assumed to satisfy the *wide-sense stationary uncorrelated scattering* (WSSUS) property. Thus, the second-order statistics of $\mathbb{H}$ are described by the *Doppler spectrum* or *scattering function* [9] $C_{\mathbb{H}}(\tau,\nu)$, where τ denotes time delay and ν denotes Doppler frequency. Practical wireless WSSUS channels are *underspread* [4,10,11], i.e., their scattering function is effectively supported within a rectangular region $\mathcal{S} \triangleq [0,\tau_{\max}] \times [-\nu_{\max},\nu_{\max}]$ of area $2\tau_{\max}\nu_{\max} \ll 1$.

Demodulator. At the receiver, the demodulator computes the inner products of $r(t)$ with time-frequency translates $\gamma_{l,k}(t) \triangleq$

$\gamma(t-lT)\,e^{j2\pi kF(t-lT)}$ of a receive pulse $\gamma(t)$, i.e.,

$$x_{l,k} \triangleq \langle r, \gamma_{l,k} \rangle = \int_t r(t)\,\gamma_{l,k}^*(t)\,dt\,. \tag{2}$$

For pulse-shaping OFDM, there is simply $\gamma(t) = g(t)$. Perfect demodulation ($x_{l,k} = a_{l,k}$ in the case of an ideal channel, i.e., for $r(t) = s(t)$) is obtained if and only if the transmit/receive pulses satisfy the *biorthogonality condition*

$$\langle g, \gamma_{l,k} \rangle = \delta_l\,\delta_k\,. \tag{3}$$

For pulse-shaping OFDM, (3) reduces to the orthogonality condition $\langle g, g_{l,k} \rangle = \delta_l\,\delta_k$. A necessary condition for (3) to hold is $TF \geq 1$. However, because the spectral efficiency is proportional to $1/(TF)$, typically TF is chosen only slightly larger than 1. In particular, practical CP-OFDM systems are designed with TF ranging from 1.03 to 1.25, corresponding to a spectral efficiency of $1/(TF) = 0.8 \ldots 0.97$. Whereas a larger TF results in a smaller spectral efficiency, it increases the freedom in designing pulses satisfying (3).

3. ISI/ICI ANALYSIS

Exact Analysis. In a pulse-shaping OFDM/BFDM system, the transmit symbols $a_{l,k}$ and the received symbols $x_{l,k}$ in (2) are related as [4]

$$x_{l,k} = \sum_{l'=-\infty}^{\infty} \sum_{k'=0}^{K-1} \langle \mathbb{H} g_{l',k'}, \gamma_{l,k} \rangle\, a_{l',k'}\,. \tag{4}$$

The terms in this sum with $l' \neq l$ and/or $k' \neq k$ describe the ISI and ICI introduced by the channel $\mathbb{H}$. A major advantage of OFDM/BFDM systems is that they allow simple scalar equalization. This is based on the approximation

$$x_{l,k} \approx H_{l,k}\,a_{l,k}\,, \qquad \text{with} \quad H_{l,k} \triangleq \langle \mathbb{H} g_{l,k}, \gamma_{l,k} \rangle\,,$$

which corresponds to neglecting the ISI/ICI terms in (4).

In what follows, we will consider the mean-square error introduced by this approximation or, equivalently, the *mean ISI/ICI power*

$$\sigma_{\mathrm{I}}^2 \triangleq \mathrm{E}\{|x_{l,k} - H_{l,k}\,a_{l,k}|^2\}\,.$$

Using the statistical independence of the symbols $a_{l,k}$, one obtains $\sigma_{\mathrm{I}}^2 = \sigma_x^2 - \sigma_{\mathrm{D}}^2$, where $\sigma_x^2 \triangleq \mathrm{E}\{|x_{l,k}|^2\}$ is the total received power and $\sigma_{\mathrm{D}}^2 \triangleq \mathrm{E}\{|H_{l,k}\,a_{l,k}|^2\}$ is the "desired" signal power. Using the WSSUS assumption, one can show that

$$\sigma_{\mathrm{D}}^2 = \sigma_a^2 \int_\tau \int_\nu C_{\mathbb{H}}(\tau,\nu)\,|A_{\gamma,g}(\tau,\nu)|^2\,d\tau\,d\nu\,, \tag{5}$$

with $A_{\gamma,g}(\tau,\nu) \triangleq \int_t \gamma(t)\,g^*(t-\tau)\,e^{-j2\pi\nu t}\,dt$ denoting the cross-ambiguity function [12] of $\gamma(t)$ and $g(t)$. Similarly, assuming an infinite number of subcarriers[1] ($k \in \mathbb{Z}$), one can show

$$\sigma_x^2 = \sigma_a^2 \int_\tau \int_\nu C_{\mathbb{H}}(\tau,\nu)\,\mathscr{A}_{\gamma,g}(\tau,\nu)\,d\tau\,d\nu\,,$$

where $\mathscr{A}_{\gamma,g}(\tau,\nu)$ is a periodized version of $|A_{\gamma,g}(\tau,\nu)|^2$, i.e.,

$$\mathscr{A}_{\gamma,g}(\tau,\nu) \triangleq \sum_{l=-\infty}^{\infty} \sum_{k=-\infty}^{\infty} |A_{\gamma,g}(\tau - lT, \nu - kF)|^2\,.$$

[1] This simplifying assumption results in an upper bound on the ISI/ICI power σ_{I}^2 obtained for finite K. This bound is quite tight for large K.

Hence, the ISI/ICI power $\sigma_{\mathrm{I}}^2 = \sigma_x^2 - \sigma_{\mathrm{D}}^2$ can be expressed as

$$\sigma_{\mathrm{I}}^2 = \sigma_a^2 \int_\tau \int_\nu C_{\mathbb{H}}(\tau,\nu)\,[\mathscr{A}_{\gamma,g}(\tau,\nu) - |A_{\gamma,g}(\tau,\nu)|^2]\,d\tau\,d\nu\,. \tag{6}$$

It follows that σ_{I}^2 will be small if $\mathscr{A}_{\gamma,g}(\tau,\nu) - |A_{\gamma,g}(\tau,\nu)|^2$ is small within the effective support region $\mathscr{S} = [0, \tau_{\max}] \times [-\nu_{\max}, \nu_{\max}]$ of $C_{\mathbb{H}}(\tau,\nu)$. This, in turn, requires that $|A_{\gamma,g}(\tau - lT, \nu - kF)|^2$ for $(l,k) \neq (0,0)$ is small within $\mathscr{S}$. Equivalently, $|A_{\gamma,g}(\tau,\nu)|^2$ has to be small within the regions $\mathscr{S}_{l,k} \triangleq [lT, lT + \tau_{\max}] \times [kF - \nu_{\max}, kF + \nu_{\max}]$ with $(l,k) \neq (0,0)$. We note that the biorthogonality relation (3) implies $A_{\gamma,g}(lT, kF) = 0$ for $(l,k) \neq (0,0)$ and thus forces $|A_{\gamma,g}(\tau,\nu)|^2$ to be zero at the center of $\mathscr{S}_{l,k}$.

Approximations and Bounds. The channel's scattering function $C_{\mathbb{H}}(\tau,\nu)$ is often not known exactly. Thus, an approximate expression of σ_{I}^2 in terms of more global and more readily available channel parameters is desirable.

Because the channel is underspread, $C_{\mathbb{H}}(\tau,\nu)$—and, thus, the integrand in (6)—is well concentrated about the origin. We can here approximate $|A_{\gamma,g}(\tau,\nu)|^2$ by the second-order Taylor series

$$|A_{\gamma,g}(\tau,\nu)|^2 \approx \sum_{n=0}^{2} \frac{1}{n!} \left(\tau \frac{\partial}{\partial \tau} + \nu \frac{\partial}{\partial \nu} \right)^n |A_{\gamma,g}(\tau,\nu)|^2 \Big|_{(\tau,\nu)=(0,0)}\,.$$

Assuming real-valued and even-symmetric pulses that satisfy $\int_t t\,\gamma(t)\,g(t)\,dt = 0$, $\int_f f\,\Gamma(f)\,G(f)\,df = 0$, and $\langle g, \gamma \rangle = 1$, this yields

$$|A_{\gamma,g}(\tau,\nu)|^2 \approx 1 - 4\pi^2 \left(B_{g,\gamma}\,\tau^2 + D_{g,\gamma}\,\nu^2 \right)\,, \tag{7}$$

where

$$D_{g,\gamma} \triangleq \int_t t^2\,g(t)\,\gamma(t)\,dt\,, \qquad B_{g,\gamma} \triangleq \int_f f^2\,G(f)\,\Gamma(f)\,df$$

are measures of the "joint" duration and bandwidth, respectively, of the transmit pulse $g(t)$ and the receive pulse $\gamma(t)$. Inserting (7) into (6) yields the approximation

$$\sigma_{\mathrm{I}}^2 \approx \sigma_a^2(\beta_1 + \beta_2)\,, \tag{8}$$

with

$$\beta_1 \triangleq 4\pi^2\,\sigma_{\mathbb{H}}^2\,(\sigma_\tau^2 B_{g,\gamma} + \sigma_\nu^2 D_{g,\gamma})\,,$$

$$\beta_2 \triangleq \int_\tau \int_\nu C_{\mathbb{H}}(\tau,\nu)\,[\mathscr{A}_{\gamma,g}(\tau,\nu) - 1]\,d\tau\,d\nu\,.$$

Here, $\sigma_{\mathbb{H}}^2 \triangleq \int_\tau \int_\nu C_{\mathbb{H}}(\tau,\nu)\,d\tau\,d\nu$ denotes the channel's path loss, and

$$\sigma_\tau^2 \triangleq \frac{1}{\sigma_{\mathbb{H}}^2} \int_\tau \int_\nu \tau^2\,C_{\mathbb{H}}(\tau,\nu)\,d\tau\,d\nu\,,$$

$$\sigma_\nu^2 \triangleq \frac{1}{\sigma_{\mathbb{H}}^2} \int_\tau \int_\nu \nu^2\,C_{\mathbb{H}}(\tau,\nu)\,d\tau\,d\nu$$

are the channel's delay spread and Doppler spread, respectively. For $\sigma_{\mathbb{H}}^2$, σ_τ^2 and σ_ν^2 given, β_1 can be interpreted as a measure of the "joint" time-frequency concentration of $g(t)$ and $\gamma(t)$. Furthermore, β_2 can be interpreted as a measure of how strongly the pulses $g(t)$ and $\gamma(t)$ deviate from those of an OFDM system. Indeed, for (pulse-shaping) OFDM satisfying

the orthogonality condition $\langle g, g_{l,k} \rangle = \delta_l \delta_k$, $\mathscr{A}_{g,g}(\tau, \nu) \equiv 1$ [13] and consequently $\beta_2 = 0$. We conclude that small ISI/ICI is achieved if $g(t)$ and $\gamma(t)$ are similar to OFDM pulses and well time-frequency localized.

If $C_{\mathrm{H}}(\tau, \nu)$ is supported within $\mathscr{S} = [0, \tau_{\max}] \times [-\nu_{\max}, \nu_{\max}]$, one can derive the even simpler upper bounds

$$\beta_1 \leq 4\pi^2 \sigma_{\mathrm{H}}^2 \left(\tau_{\max}^2 B_{g,\gamma} + \nu_{\max}^2 D_{g,\gamma}\right),$$
$$\beta_2 \leq \sigma_{\mathrm{H}}^2 \max_{(\tau,\nu)\in\mathscr{S}} \left|\mathscr{A}_{\gamma,g}(\tau, \nu) - 1\right|,$$

which depend only on the global channel parameters $\tau_{\max}$, $\nu_{\max}$, σ_{H}^2 and on the pulses $g(t)$, $\gamma(t)$.

For a conventional CP-OFDM system with a cyclic-prefix length T_{cp} that is larger than the channel's maximum delay, (8) can be shown to simplify to $\sigma_{\mathrm{I}}^2 \approx \frac{\pi^2}{3} \sigma_{\mathrm{H}}^2 \sigma_{\nu}^2 (T - T_{\mathrm{cp}})^2$. This expression generalizes results obtained for Jakes and uniform Doppler spectra [14] and for "frequency offset" channels [15].

4. OPTIMAL PULSE DESIGN

We now present two methods for designing the pulses $g(t), \gamma(t)$ such that the ISI/ICI power σ_{I}^2 is minimized. These methods are based on the following alternative expression of σ_{I}^2 [4]:

$$\sigma_{\mathrm{I}}^2 = \sigma_{\mathrm{I}}^2(g, \gamma) = \sigma_a^2 \int_{\tau} \int_{\nu} \mathscr{C}_{\mathrm{H}}(\tau, \nu) \left|A_{\gamma,g}(\tau, \nu)\right|^2 d\tau d\nu, \quad (9)$$

with

$$\mathscr{C}_{\mathrm{H}}(\tau, \nu) \triangleq \sum_{l\neq 0} \sum_{k\neq 0} C_{\mathrm{H}}(\tau - lT, \nu - kF).$$

Note that $\mathscr{C}_{\mathrm{H}}(\tau, \nu)$ is a periodized scattering function with the $l = k = 0$ component $C_{\mathrm{H}}(\tau, \nu)$ omitted. If the scattering function is not known, or if good pulses for a whole range of scattering functions are to be found, one may use a default $C_{\mathrm{H}}(\tau, \nu)$ that is constant on $\mathscr{S} = [0, \tau_{\max}] \times [-\nu_{\max}, \nu_{\max}]$ and zero outside $\mathscr{S}$. This merely requires specification of the maximum delay $\tau_{\max}$ and the maximum Doppler $\nu_{\max}$.

First Design Method. Our first pulse design method presupposes a prescribed transmit pulse $g^{(0)}(t)$. The ISI/ICI power $\sigma_{\mathrm{I}}^2(g^{(0)}, \gamma)$ is minimized with respect to the receive pulse $\gamma(t)$, subject to the biorthogonality condition (3). This is possible because for a fixed $g(t)$ and $TF > 1$, $\gamma(t)$ is not uniquely determined by (3). Using results from Weyl-Heisenberg frame theory [12], it can be shown that all receive pulses satisfying (3) for the given $g^{(0)}(t)$ can be written as [12, p. 142]

$$\gamma(t) = \gamma^{(0)}(t) + \sum_i c_i u_i(t), \quad (10)$$

where $\gamma^{(0)}(t)$ is the so-called "canonical dual" of $g^{(0)}(t)$, $\{u_i(t)\}$ is an orthonormal basis determined by $g^{(0)}(t)$ (more precisely, an orthonormal basis of the orthogonal complement of the space spanned by $\{g_{l,k}^{(0)}(t)\}$), and the c_i are arbitrary coefficients. Using (10), the constrained minimization of $\sigma_{\mathrm{I}}^2(g^{(0)}, \gamma)$ becomes equivalent to an *unconstrained* minimization with respect to the coefficients c_i. The ISI/ICI power $\sigma_{\mathrm{I}}^2(g^{(0)}, \gamma)$ is a quadratic functional of the c_i. It can thus be shown that this minimization amounts to solving the system of linear equations[2] $\mathbf{Bc} = -\mathbf{a}$, where $[\mathbf{c}]_i = c_i$ and

$$[\mathbf{B}]_{i,j} = \int_{\tau} \int_{\nu} \mathscr{C}_{\mathrm{H}}(\tau, \nu) A^*_{u_i, g^{(0)}}(\tau, \nu) A_{u_j, g^{(0)}}(\tau, \nu) d\tau d\nu,$$
$$[\mathbf{a}]_i = \int_{\tau} \int_{\nu} \mathscr{C}_{\mathrm{H}}(\tau, \nu) A^*_{u_i, g^{(0)}}(\tau, \nu) A_{\gamma^{(0)}, g^{(0)}}(\tau, \nu) d\tau d\nu.$$

Hence, the optimal biorthogonal receive pulse is given by $\gamma^{\mathrm{opt}}(t) = \gamma^{(0)}(t) + \sum_i c_i^{\mathrm{opt}} u_i(t)$, where $c_i^{\mathrm{opt}} = [\mathbf{c}^{\mathrm{opt}}]_i$ with $\mathbf{c}^{\mathrm{opt}} = -\mathbf{B}^{-1}\mathbf{a}$. The same approach can be used to optimize the transmit pulse $g(t)$ for a prescribed receive pulse $\gamma^{(0)}(t)$.

Second Design Method. To further reduce the ISI/ICI power, we next propose to minimize σ_{I}^2 normalized by $\sigma_{\mathrm{D}}^2 = \mathrm{E}\{|H_{l,k} a_{l,k}|^2\}$ with respect to *both* $g(t)$ and $\gamma(t)$ simultaneously. Thus, the cost function to be minimized is $J(g, \gamma) \triangleq \sigma_{\mathrm{I}}^2 / \sigma_{\mathrm{D}}^2$, with σ_{I}^2 and σ_{D}^2 given by (9) and (5), respectively. Note that $J(g, \gamma)$ is the reciprocal of the signal-to-interference ratio (SIR) $\sigma_{\mathrm{D}}^2 / \sigma_{\mathrm{I}}^2$. The biorthogonality constraint is now dropped for the sake of increased pulse design freedom. Thus, the optimized pulses will not be exactly biorthogonal, which means that some ISI/ICI will occur even for an ideal channel. However, this is not a problem because an ideal channel never occurs in practice. Moreover, we observed that the optimized pulses tend to be almost biorthogonal.

Because $J(g, \gamma)$ depends nonquadratically on $g(t)$, $\gamma(t)$, we use the numerical minimization function *fminunc* from MATLAB's optimization toolbox. In general, the resulting "optimal" pulses merely correspond to a local minimum of $J(g, \gamma)$ instead of the global minimum desired, and they depend on the pulses used for initializing the minimization.

Simulation results for both design methods will be presented in Section 6.

5. EFFICIENT IMPLEMENTATION

We next propose an efficient digital implementation of the modulator and demodulator in a pulse-shaping OFDM/BFDM system. We assume that all signals are sampled at a rate that is equal to the system bandwidth KF. In the resulting discrete-time, normalized-frequency setting, the subcarrier spacing is $1/K$ and the discrete symbol duration is $N = KTF$. The sampled transmit and receive pulses are assumed to have finite length which will be denoted by L_g and L_γ, respectively.

As shown in Fig. 1, the proposed implementations essentially consist of the usual length-K IDFT or DFT that is also required in CP-OFDM systems, a pulse-shaping operation (elementwise multiplication by the vector $\mathbf{g} = (g[0] \cdots g[L_g - 1])^T$ or $\boldsymbol{\gamma} = (\gamma[0] \cdots \gamma[L_\gamma - 1])^T$), and an overlap/add or pre-aliasing operation. We note that in practically relevant scenarios where $TF = N/K$ is only slightly larger than 1, polyphase implementations [16] are not possible since they would require TF to be an integer.

Modulator. The digital OFDM/BFDM modulator computes the transmit signal (cf. (1))

$$s[n] = \frac{1}{\sqrt{K}} \sum_{l=-\infty}^{\infty} \sum_{k=0}^{K-1} a_{l,k}\, g[n - lN]\, e^{j2\pi \frac{k}{K}(n - lN)}.$$

[2] In practical digital implementations, the matrix $\mathbf{B}$ and the vectors $\mathbf{a}$ and $\mathbf{c}$ are finite-dimensional.

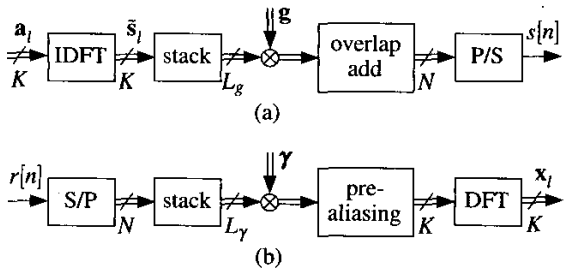

Figure 1: *Efficient digital implementation of a pulse-shaping OFDM/BFDM system: (a) Modulator, (b) demodulator.*

Within the lth symbol period, $s[n]$ can be written as

$$s[n] = \sum_{i=l-Q_g}^{l+Q_g} s_i^{(g)}[n-iN], \quad n \in [lN,(l+1)N-1], \qquad (11)$$

where $Q_g = \lceil L_g/(2N) \rceil$ and

$$s_l^{(g)}[n] = \tilde{s}_l[n]\,g[n], \quad \text{with } \tilde{s}_l[n] = \frac{1}{\sqrt{K}} \sum_{k=0}^{K-1} a_{l,k}\, e^{j2\pi \frac{nk}{K}}. \qquad (12)$$

Equation (11) describes an overlap/add operation that involves $2Q_g+1$ windowed IDFT signals $s_l^{(g)}[n]$ (see (12)). These can be computed by periodically repeating (stacking) the vector $\tilde{\mathbf{s}}_l = (\tilde{s}_l[0] \cdots \tilde{s}_l[K-1])^T$ containing the length-K normalized IDFT of the $a_{l,k}$ to form a length-L_g vector. Subsequently, this vector is multiplied elementwise by the transmit pulse vector $\mathbf{g}$. The resulting efficient implementation of the modulator is shown in Fig. 1(a).

Demodulator. At the receiver, demodulation of the received signal $r[n]$ is performed according to (cf. (2))

$$x_{l,k} = \frac{1}{\sqrt{K}} \sum_{n=-\infty}^{\infty} r[n]\,\gamma^*[n-lN]\, e^{-j2\pi \frac{k}{K}(n-lN)}.$$

This can be efficiently implemented by means of the length-K normalized DFT

$$x_{l,k} = \frac{1}{\sqrt{K}} \sum_{n=0}^{K-1} \tilde{r}_l^{(\gamma)}[n]\, e^{-j2\pi \frac{kn}{K}}.$$

Here, the length-K sequence $\tilde{r}_l^{(\gamma)}[n]$ is obtained from the windowed received signal $r_l^{(\gamma)}[n] \triangleq r[n+lN]\,\gamma^*[n]$ via the "pre-aliasing" operation

$$\tilde{r}_l^{(\gamma)}[n] = \sum_{i=-Q_\gamma}^{Q_\gamma} r_l^{(\gamma)}[n+iK],$$

with $Q_\gamma = \lceil L_\gamma/(2K) \rceil$. This leads to the efficient demodulator implementation sketched in Fig. 1(b).

Computational Complexity. The complexity of the modulator is determined by the IDFT and the pulse shaping, requiring a total of $\mathcal{O}(K\log_2 K + L_g)$ operations per symbol period. Similarly, the DFT and windowing at the receiver amount to $\mathcal{O}(K\log_2 K + L_\gamma)$ operations per symbol period. Compared to a CP-OFDM system that requires only the IDFT/DFT (i.e., no pulse-shaping), this is an increase by $L_g + L_\gamma$ operations per symbol period. As an example, for a BFDM system with $K = 1024$ carriers, symbol length $N = 1280$, and pulse length $L_g = L_\gamma = 2N$, the increase in computational complexity with respect to a CP-OFDM system is only 25%. We note that due to the overlap/add and pre-aliasing operations, pulse-shaping OFDM/BFDM systems require additional memory and introduce a latency of a few symbol periods.

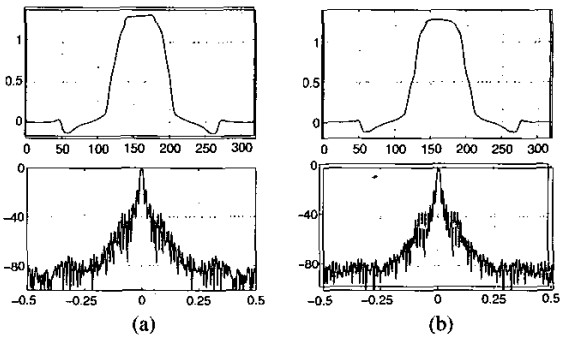

Figure 2: *Pulse shape (top) and Fourier transform magnitude (bottom, in dB) of (a) the transmit pulse and (b) the receive pulse of the BFDM system $\mathscr{G}_{\text{II}}$.*

6. SIMULATION RESULTS

BFDM System Design. We consider four BFDM systems and a reference CP-OFDM system with transmit bandwidth $KF = 1\,\text{MHz}$, $K = 64$ subcarriers, symbol duration $T = 80\,\mu\text{s}$, and subcarrier spacing $F = 15.625\,\text{kHz}$. We thus have $TF = 1.25$, which corresponds to a spectral efficiency parameter of $1/(TF) = 0.8$. Assuming a sampling frequency of 1 MHz, we obtain the discrete-time symbol duration as $N = 80$. The cyclic prefix of the CP-OFDM system has length $16\,\mu\text{s}$. The pulse length of the BFDM systems is $L = L_g = L_\gamma = 320$. The scattering function used for the BFDM pulse design is constant on $\mathscr{S} = [0, \tau_{\max}] \times [-\nu_{\max}, \nu_{\max}]$ with $\tau_{\max} = 8\,\mu\text{s}$ and $\nu_{\max} = 625\,\text{Hz}$ and zero outside $\mathscr{S}$.

We designed two BFDM systems, denoted by $\mathscr{G}_{\text{I}}$ and $\mathscr{R}_{\text{I}}$, by prescribing a (truncated) Gaussian transmit pulse and a rectangular transmit pulse, respectively and computing the optimal receive pulse using the first design method from Section 4. Two further BFDM systems $\mathscr{G}_{\text{II}}$ and $\mathscr{R}_{\text{II}}$ were designed using the second design method from Section 4. Here, the minimization procedure was initialized by a Gaussian transmit pulse ($\mathscr{G}_{\text{II}}$) and a rectangular transmit pulse ($\mathscr{R}_{\text{II}}$) and the associated canonical duals for the receive pulses.

For illustration, the transmit and receive pulses of $\mathscr{G}_{\text{II}}$ are shown in Fig. 2. It is seen that both pulses consist of a main lobe of width $\approx N$ and small sidelobes. The two pulses are very similar, which means that $\mathscr{G}_{\text{II}}$ is almost an OFDM system (the angle between $g[n]$ and $\gamma[n]$ is about 7.5°, as compared to 0° for pulse-shaping OFDM). This is important because a BFDM system in which $\gamma[n]$ is very different from $g[n]$ may suffer from noise enhancement at the receiver [4].

SIR Performance. Fig. 3 shows the SIR $\sigma_{\text{D}}^2/\sigma_{\text{I}}^2$ obtained with our BFDM systems and with the reference CP-OFDM

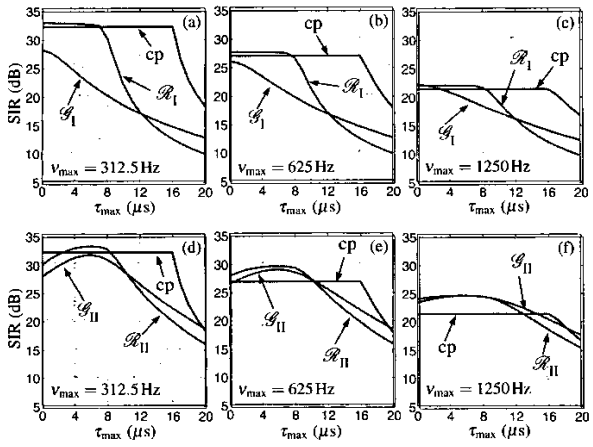

Figure 3: *SIR obtained with the four BFDM systems $\mathscr{G}_{\rm I}, \mathscr{R}_{\rm I}, \mathscr{G}_{\rm II}$, and $\mathscr{R}_{\rm II}$ and the CP-OFDM system (denoted "cp"): (a)–(c) $\mathscr{G}_{\rm I}$, $\mathscr{R}_{\rm I}$, and cp; (d)–(f) $\mathscr{G}_{\rm II}$, $\mathscr{R}_{\rm II}$, and cp.*

system for different channel scattering functions. These scattering functions are constant on $\mathscr{S} = [0, \tau_{\max}] \times [-\nu_{\max}, \nu_{\max}]$ and zero outside $\mathscr{S}$, with $\tau_{\max}$ ranging from 0 to 20 μs and $\nu_{\max} \in \{312.5\,\text{Hz}, 625\,\text{Hz}, 1250\,\text{Hz}\}$. Note that the scattering functions are generally different from those for which our pulses were designed (for pulse design, we used $\tau_{\max} = 8\,\mu$s and $\nu_{\max} = 625\,$Hz), thus assessing the robustness of our designs. It is seen that the SIR of $\mathscr{G}_{\rm I}$ is smaller than that of CP-OFDM for virtually all channel parameters, and the SIR of $\mathscr{R}_{\rm I}$ is just slightly larger than that of CP-OFDM for $\tau_{\max} \leq 8\,\mu$s and all $\nu_{\max}$. On the other hand, the BFDM systems $\mathscr{G}_{\rm II}$ and $\mathscr{R}_{\rm II}$ achieve an SIR improvement of up to about 3 dB over the CP-OFDM system in certain ranges of $\tau_{\max}$ and $\nu_{\max}$.

To further illustrate this potential SIR advantage of BFDM, Fig. 4 identifies the regions in the $(\tau_{\max}, \nu_{\max})$-plane where the best SIR performance is achieved by $\mathscr{G}_{\rm II}$ (light grey), $\mathscr{R}_{\rm II}$ (dark grey), and CP-OFDM (white). It is seen that the BFDM systems $\mathscr{G}_{\rm II}$ and $\mathscr{R}_{\rm II}$ outperform CP-OFDM for a wide range of channel parameters, especially for large Doppler frequencies, i.e., fast time-varying channels.

7. CONCLUSIONS

We presented an ISI/ICI-optimal design of the transmit and receive pulses of BFDM systems operating over time-varying channels. Using this design, we demonstrated that for realistic values of spectral efficiency and for fast time-varying channels (i.e., large Doppler), the SIR of BFDM systems can be larger than that of conventional CP-OFDM systems by about 3 dB. We also presented an ISI/ICI analysis of pulse-shaping OFDM/BFDM systems, as well as efficient FFT-based modulator and demodulator implementations that are only slightly more complex than those of CP-OFDM systems.

ACKNOWLEDGMENT

The authors are grateful to K. Gröchenig and H. G. Feichtinger for stimulating discussions.

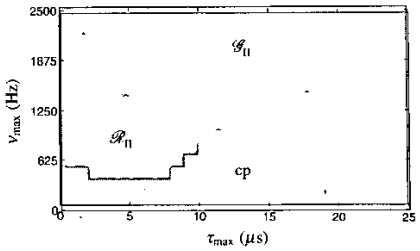

Figure 4: *Regions in the (τ_{max}, ν_{max})-plane where $\mathscr{G}_{\rm II}$, $\mathscr{R}_{\rm II}$, and CP-OFDM (cp) outperform the respective other systems.*

REFERENCES

[1] R. W. Chang, "Synthesis of band-limited orthogonal signals for multi-channel data transmission," *Bell Syst. Tech. J.*, vol. 45, pp. 1775–1796, Dec. 1966.

[2] A. Peled and A. Ruiz, "Frequency domain data transmission using reduced computational complexity algorithms," in *Proc. IEEE ICASSP-80*, (Denver, CO), pp. 964–967, 1980.

[3] P. Smulders, "Exploiting the 60 GHz band for local wireless multimedia access: Prospects and future directions," *IEEE Comm. Mag.*, pp. 140–147, Jan. 2002.

[4] W. Kozek and A. F. Molisch, "Nonorthogonal pulseshapes for multicarrier communications in doubly dispersive channels," *IEEE J. Sel. Areas Comm.*, vol. 16, pp. 1579–1589, Oct. 1998.

[5] P. K. Remvik and N. Holte, "Carrier frequency offset robustness for OFDM systems with different pulse shaping filters," in *Proc. IEEE GLOBECOM-97*, (Phoenix, AZ), pp. 11–15, 1997.

[6] A. Vahlin and N. Holte, "Optimal finite duration pulses for OFDM," *IEEE Trans. Comm.*, vol. 4, pp. 10–14, Jan. 1996.

[7] R. Haas and J. C. Belfiore, "A time-frequency well-localized pulse for multiple carrier transmission," *Wireless Personal Comm.*, vol. 5, pp. 1–18, 1997.

[8] H. Bölcskei, "Efficient design of pulse shaping filters for OFDM systems," in *Proc. SPIE Wavelet Applications in Signal and Image Processing VII*, (Denver, CO), pp. 625–636, July 1999.

[9] P. A. Bello, "Characterization of randomly time-variant linear channels," *IEEE Trans. Comm. Syst.*, vol. 11, pp. 360–393, 1963.

[10] J. G. Proakis, *Digital Communications*. New York: McGraw-Hill, 3rd ed., 1995.

[11] F. Hlawatsch and G. Matz, "Time-frequency characterization of random channels," in *Time-Frequency Signal Analysis and Processing* (B. Boashash, ed.), Englewood Cliffs (NJ): Prentice Hall, 2002.

[12] K. Gröchenig, *Foundations of Time-Frequency Analysis*. Boston: Birkhäuser, 2001.

[13] R. Tolimieri and R. S. Orr, "Characterization of Weyl-Heisenberg frames via Poisson summation relationships," in *Proc. IEEE ICASSP-92*, (San Francisco, CA), pp. 277–280, March 1992.

[14] Y. Li and L. Cimini, "Bounds on the interchannel interference of OFDM in time-varying impairments," *IEEE Trans. Comm.*, vol. 49, pp. 401–404, March 2001.

[15] T. Pollet, M. V. Bladel, and M. Moeneclaey, "BER sensitivity of OFDM systems to carrier frequency offset and Wiener phase noise," *IEEE Trans. Comm.*, vol. 43, pp. 191–193, Feb. 1995.

[16] P. P. Vaidyanathan, *Multirate Systems and Filter Banks*. Englewood Cliffs (NJ): Prentice Hall, 1993.